Published in final edited form as:
Clin Radiol. 2012 January ; 67(1): 38–46. doi:10.1016/j.crad.2011.03.023.

CT features and quantification of the characteristics of adrenocortical carcinomas on unenhanced and contrast-enhanced studies

H.M. Zhang[a,b], **N.D. Perrier**[c], **E.G. Grubbs**[c], **K. Sircar**[d], **Z.X. Ye**[a,e], **J.E. Lee**[c], and **C.S. Ng**[a,*]

[a]Department of Radiology, The University of Texas MD Anderson Cancer Center, Houston, TX, USA

[b]Department of Diagnostic Radiology, Cancer Hospital and Institute, Chinese Academy of Medical Sciences, Peking Union Medical College, Beijing, China

[c]Department of Surgical Oncology, The University of Texas MD Anderson Cancer Center, Houston, TX, USA

[d]Department of Pathology, The University of Texas MD Anderson Cancer Center, Houston, TX, USA

[e]Department of Radiology, Tianjin Medical University Cancer Institute and Hospital, Tianjin, China

Abstract

AIM—To describe the morphological and contrast-agent washout characteristics of adrenocortical carcinomas (ACCs) on computed tomography (CT).

MATERIALS AND METHODS—Forty-one patients with histopathologically proven ACCs were retrospectively evaluated. The morphological characteristics of the ACCs were documented and compared with surgical and histopathological findings. The percentage of contrast agent enhancement washout (PEW) and relative PEW (RPEW) were calculated for 17 patients who had the combination of unenhanced, portal venous, and 15 min delayed phase images.

RESULTS—Characteristic imaging findings of ACCs included large size (38 of 41 tumours were >6 cm), well-defined margin with a thin enhancing rim (25 patients), and central stellate area of low attenuation on contrast-enhanced CT images (21 patients). Tumour extension into the inferior vena cava (IVC) with associated thrombus was identified on CT in six (14.6%) patients. Of 17 tumours evaluated, 12 (71%) had a PEW value of ≤60%, and 14 (82%) had an RPEW value of ≤40%.

CONCLUSION—Large size, a well-defined margin with a thin enhancing rim, central low attenuation, and a predilection for extension into the IVC are typical morphological characteristics of ACC on CT. The contrast-washout characteristics of ACCs, in concordance with their malignant nature, share those of non-adenomas rather than adenomas.

Introduction

Adrenocortical carcinoma (ACC) is a rare, highly malignant neoplasm with a poor prognosis. ACCs are reported to occur in less than two cases per million annually in the US,

*Guarantor and correspondent: C.S. Ng, Department of Diagnostic Radiology - Unit 1473, The University of Texas MD Anderson Cancer Center, 1400 Pressler St, Houston, TX 77030-4009, USA. Tel.: +1 (713) 792 6759; fax: +1 (713) 745 1302. cng@mdanderson.org (C.S. Ng).

resulting in less than 0.2% of cancer deaths.[1–3] The mean overall survival in patients with unresectable tumours is only 6 months; however, the overall 5-year survival for patients who undergo complete resection is 32–48%.[4,5] Abdominal imaging, especially computed tomography (CT), has an important role in detection of ACC, staging, evaluation for resectability, and surgical treatment planning as the ability to perform total excision is the most important positive prognostic factor.[2–5]

Previous descriptions of the radiological appearances of ACC have focused on the tumour's internal morphological characteristics.[6,7] There have been relatively few radiological evaluations of the tumour's invasive properties, for example, invasion into adjacent organs and vasculature; and these have only been small series consisting of one to 15 patients.[8–10] Although there is substantial literature regarding the use of quantitative CT for evaluation of adrenal tumours, especially the importance of unenhanced Hounsfield densities and contrast medium washout characteristics, these reports have largely focused their attention on the differentiation of adrenal adenomas from non-adenomas.[11–14] There are few reports evaluating these characteristics in ACCs.[15,16]

Therefore, the purpose of the present study was to evaluate and quantify the morphological and contrast-enhanced CT characteristics of a large series of histopathologically proven ACCs, including size, attenuation, invasion, metastasis, and contrast medium washout.

Materials and methods

Patients

The institutional review board approved this HIPAA-compliant retrospective study and waived the need for informed consent. Computerized institutional pathology and radiology databases were searched to identify patients who had a histopathologically confirmed diagnosis of ACC and had undergone abdominal CT imaging before any treatment, from 1 January 2001 to 31 August 2009. In total, 41 ACCs in 41 patients were identified: 17 men and 24 women, with a mean age of 52.3 years (range 15.9–80.8 years). Nineteen tumours arose in the right adrenal gland and 22 in the left. Adrenalectomy was performed in 34 patients; the other seven patients did not undergo surgery, the pathological diagnosis being established by biopsy of their primary tumour.

The presenting symptoms and signs in these 41 patients included: Cushing's syndrome (n = 9, including three with virilization); hyperaldosteronism (n = 3), bilateral lower-extremity oedema (n = 3); left varicocele (n = 2); hypertension (n = 2); and cough related to lung metastases (n = 1). Seventeen patients had non-specific symptoms, including abdominal discomfort; flank or back pain related to local mass effect; and four patients were asymptomatic.

CT acquisition

The majority (34 of 41) of the CT images for review had been undertaken at our institution. Images were obtained with a variety of multidetector row helical CT systems (LightSpeed QX/I, n = 7; LightSpeed Plus, n = 3; LightSpeed 16, n = 17; or LightSpeed VCT, n = 7; GE Healthcare, Milwaukee, WI, USA; and other CT systems, n = 7). CT parameters for all images reviewed included: 120–140 kV; 180–440 mA; 0.9375:1 pitch for LightSpeed 16, 0.984375:1 pitch for LightSpeed VCT, and 1:1 pitch for LightSpeed QX/I, LightSpeed Plus, and the other systems; 2.5–5mm collimation; and a standard soft-tissue reconstruction algorithm. Intravenous (IV) contrast-enhanced imaging at our institution was undertaken with IV administration of 100–120 ml of a non-ionic contrast agent [iohexol 100 mg iodine/

ml (Omnipaque 300) or iodixanol 320 mg iodine/ml (Visipaque 320); GE Healthcare] via a power injector at the rate of 2–2.5 ml/s.

A variety of combinations of unenhanced and intravenous (IV) contrast-enhanced images were available for review. Both unenhanced and contrast-enhanced images were available for 37 of the 41 patients; isolated unenhanced images were available for two others, and for the remaining two, only contrast-enhanced images. Among the 39 patients who had contrast-enhanced CT images, the following phases were available for review: arterial phase (30–35 s delay) in 24; portal venous phase (60–70 s delay) in 37; 3 min delayed in 13; and 15 min delayed in 19. Among the latter 19 patients, the combination of unenhanced, portal venous, and 15 min delayed images were available in 17.

Image analysis

The primary analysis of images was undertaken on studies obtained prior to any form of treatment, in order to limit the confounding effects of therapies on the tumour(s). For the majority of patients, this represented their presenting CT imaging: only 13 of the 41 patients had any prior abdominal imaging. Of these 13 patients, there was only one with a remote CT (3.5 years), the remaining 12 had only short intervals between the index CT and their earliest available CT (median 47 days, range 8–76 days).

For the 34 patients who underwent adrenalectomy, the median interval between their initial pretreatment CT and resection was 20 days (range 1–69 days). Three of these 34 patients underwent neoadjuvant chemotherapy ($n = 2$) and trans-arterial chemo-embolization (TACE; $n = 1$).

All archived CT images for the 41 patients were transferred to an Advantage Workstation 4.0 (GE Healthcare). Two radiologists (one with 20 and one with 11 years experience in body CT imaging) evaluated the images for morphological characteristics, and discrepancies were resolved by consensus.

The following qualitative morphological characteristics of the primary tumour were documented: size (maximum axial diameter), shape (round or oval versus lobulate), margin definition (well defined versus ill defined), rim enhancement (present versus absent), attenuation appearance (homogeneous versus heterogeneous), and calcification (present versus absent). In addition, the presence or absence of hypoattenuating areas was noted; and if present, whether the area was stellate or irregular in morphology.

Besides these features of the primary tumour, the presence or absence of organ invasion, venous thrombus, lymphadenopathy, and distant metastases were also evaluated, and compared with surgical and pathological results. Calcification was considered to be present if there was a region with attenuation greater than 120 HU on unenhanced images. Organ invasion was considered to be present on CT if the fat plane between the tumour and the adjacent organ was obliterated and the density of the adjacent structure was attenuated. Lymph node metastases were considered to be present on CT if a cluster of three or more perilesional nodes (of any size) was identified or if there were fewer than three unclustered lymph nodes of at least 10 mm in short-axial diameter.[17,18]

For quantitative analysis, one radiologist measured the size and attenuation value of tumours. The image that contained the maximum axial cross-sectional area of the tumour was used for measuring both the maximal diameter and mean attenuation value. The region of interest (ROI) was carefully hand drawn over the mass and placed at the same level for each phase of the study. As has been done in previous evaluations of the percentage of contrast agent enhancement washout (PEW) in adrenal tumours,[11,13–16] the ROI was as

large as possible while avoiding the lesion's edges to preclude partial volume effects. Areas of calcification, fat, and blood vessels were excluded where possible (Fig 1).

A variety of staging investigations had also been undertaken in the 41 patients, and all of these studies were reviewed and their findings documented: chest CT (n = 31), chest radiography (n = 34), bone scintigraphy (n = 20), and 2-[^{18}F]-fluoro-2-deoxy-D-glucose (FDG) positron-emission tomography (PET) combined with CT (n = 5).

Contrast-agent washout calculation

For the 17 patients for whom the combination of unenhanced, contrast-enhanced portal venous phase images, and 15 min delayed images were available, PEW was calculated as follows:

$$PEW = [(A_E - A_D)/(A_E - A_N] \cdot 100,$$

where A_D is the attenuation on the 15 min delayed contrast-enhanced CT image, A_E is the attenuation on the portal venous phase contrast-enhanced CT image, and A_N is the attenuation on the unenhanced CT image.[11–15] The relative percentage of contrast agent enhancement washout (RPEW) was calculated as follows (Fig 1):

$$RPEW = [(A_E - A_D)/(A_E] \cdot 100$$

Results

The relationships between tumour size and other morphological characteristics evaluated on CT are listed in Table 1.

Size

The mean (± SD) maximum axial diameter of all tumours was 11 ± 4 cm (range 4.7–22.2 cm). Thirty-eight had maximal diameters greater than 6 cm; the other three tumours had maximal diameters of 4.7, 5.5, and 6 cm. The patient with the tumour that was 5.5 cm at the time of surgical resection had undergone CT examinations 8 and 3.5 years previously, when the stability of a 1.8 cm adrenal nodule during that interval had been documented.

Shape and margin

Eleven of the 41 tumours were round or oval, and 30 were lobulate. Twenty-nine tumours had well-defined margins and 12 had ill-defined margins. Twenty-five of those 29 tumours with well-defined margins were surrounded to some degree by a thin, well-defined enhancing rim.

Internal structure

All 39 tumours with contrast-enhanced CT images demonstrated a heterogeneous enhancement pattern. On unenhanced CT, 33 tumours showed heterogeneous density and six homogeneous density. Fifteen of 41 (37%) tumours had punctate, patchy, or nodular calcification (Fig 2). All 41 tumours contained hypoattenuating areas on unenhanced and/or contrast-enhanced CT images, which were classified as central stellate (n = 21) or irregular (n = 20).

Foci of mature fat, with attenuation values varying from −41 HU to −81 HU, were observed in the centre of four tumours (Fig 3). Histopathologically, no myelolipoma or other collision tumours containing fat were identified in the two specimens with fat foci that underwent adrenalectomy (full histopathological evaluation was not available in the other two tumours as they only underwent biopsy).

Adjacent organ invasion

Adjacent organ invasion was considered to be present on the CT images in seven of the 41 patients including: liver invasion in two patients; kidney invasion in two patients; combined liver and kidney invasion in two patients; and combined pancreas, stomach, and diaphragm invasion in one patient. These patients had undergone contrast-enhanced CT and their tumours were greater than 6 cm. Adjacent organ invasion was confirmed in four of these seven patients at surgery and histopathology, including the patient with triple-organ involvement described above (the other three patients did not undergo surgery).

For the four patients who were considered to have local liver invasion, all the primary tumours were located on the right side. Invasion was confirmed in one patient who underwent resection (the other three patients did not undergo surgery). Of note, contrast-enhanced CT, which was under-taken 7 days before surgery, failed to detect, even in retrospect, the right hepatic lobe involvement in one patient who underwent surgery; this was a right-sided primary tumour and the smallest tumour in the present series (4.7 cm).

For the four patients who were considered to have adjacent kidney involvement, three were right-sided and one left-sided. Invasion was confirmed in two patients who underwent resection (the other two patients did not undergo surgery).

Venous thrombus

ACCs that extended into the inferior vena cava (IVC) with associated thrombus were detected in six of the 41 (15%) patients on CT. The primary tumour was right-sided in four of those patients and left-sided in two. In the two patients with left-sided ACCs, the tumour extended into the left renal vein and then crossed the midline into the IVC. In one of these two patients, a large tumour thrombus extended inferiorly along the gonadal vein to the lower abdomen (Figs 4 and 5).

In these six patients, tumour thrombus was confirmed by surgery and pathology in three patients (the other three patients did not undergo surgery). Of note, contrast-enhanced CT failed to prospectively identify a small non-occlusive thrombus in the left renal vein and IVC in one patient with a 14 cm tumour who underwent surgery. On retrospective review, the CT examination, which was undertaken 25 days before surgery, was noted to have been a uniphasic study obtained in a suboptimal (relatively arterial) phase of post-contrast enhancement.

Lymphadenopathy and visceral metastases

Metastatic retroperitoneal lymphadenopathy was considered to be present at CT in four patients, which was confirmed histopathologically in two patients. An inflammatory reaction was found on histopathology in a third patient, and the fourth did not undergo surgery. Among the other 31 patients who had adrenalectomies, metastatic lymphadenopathy was histopathologically detected in one patient who did not meet the CT criteria for metastatic adenopathy; the size of this primary tumour was 17 cm.

Visceral metastases were considered to be present on radiography, bone scintigraphy, CT, and/or PET-CT evaluation in six patients: three in the liver, two in the lung, and one in both the liver and bone. The four patients who were considered to have liver metastases (these were focal parenchymal lesions, as distinct from local invasion from adjacent tumour) had right-sided primary tumours; the two with lung metastases had left-sided tumours. The primary tumours in these six patients were greater than 9 cm.

Attenuation and contrast-agent washout

The mean (± SD) tumour ROI area was 20.9 ± 16.4 cm^2 (range 4–64.4 cm^2). The 39 tumours with unenhanced CT images available had a mean (± SD) attenuation value of 37.1 ± 7.2 HU; on enhanced images, the values were 68.3 ± 21.5 HU for the 24 tumours with arterial phase images; 84.1 ± 22.4 HU for the 37 tumours with portal venous phase; 73.2 ± 13.9 HU for the 13 tumours with 3 min delayed; and 62.5 ± 11.2 HU for the 19 tumours on 15 min delayed images. A summary of these enhancement characteristics is presented in Fig 6.

The mean (± SD) PEW and RPEW values for the 17 ACCs with the appropriate three phases of contrast enhancement were 50 ± 16.9% (range 6.3–72.5%) and 26.9 ± 11.4% (range 3–42.9%).

Fig 7 summarizes tumour distribution according to PEW and RPEW values. Twelve of these 17 (71%) tumours had a PEW value of 60% or less; 14 of the 17 (82%) tumours had an RPEW of less than 40%. These cut-off threshold values of PEW and RPEW have been commonly applied in previous studies for distinguishing between adrenal adenomas and non-adenomas (namely, lesions with a PEW ≤60% or RPEW ≤40% are considered to be non-adenomas).[11–13]

Discussion

Size is a commonly used characteristic in the differentiation of adrenal tumours. A review of six published reports showed that 92% (105/114) of ACCs had diameters larger than 6 cm.[19] In one series of 210 patients with incidental findings of an adrenal mass, a 5 cm cut-off yielded sensitivity for ACC of 93% and a specificity of 63%.[20] The overlapping sizes of ACCs with other non-adenomas, such as metastases and pheochromocytomas, resulted in the relatively low specificity in that study, which has also been reported by other authors.[21–25] Although size remains an important criterion for differentiating between benign and malignant adrenal lesions, size alone is insufficient for differentiating ACCs from other adrenal tumours. In the present study, the majority (38 of 41 [93%]) of the patients had ACCs larger than 6 cm, but three patients had tumours smaller than or equal to 6 cm. It is also possible that previous studies and the present study are affected by bias related to tumour size, as small adrenal tumours may simply be managed relatively conservatively (namely by surveillance), while larger tumours may undergo biopsy or surgery more expeditiously.

Calcification and a hypoattenuated or unenhanced central area have also been proposed as typical signs of ACCs.[7,8,26] In the present series, punctate, patchy, or irregularly nodular calcification was present in 37% (15 of 41), and central low-attenuation areas were found in all of the tumours. A central stellate area of low attenuation was found in more than half the tumours in the present series. This feature has been described by Ribeiro et al.[8] as resembling the central scar seen in primary liver tumours. However, as noted by Fishman et al.[7] it is also seen in pheochromocytomas, large metastases, and even adenomas, and so cannot be used as a distinguishing characteristic.

Although some fat content can be expected in ACCs, areas of macroscopic fat are extremely rare. A very small amount of mature fat was demonstrated in two of the tumours in the present study. To the authors' knowledge, only two cases of ACC containing mature fat on CT imaging have previously been reported.[27,28] The origin of intra-tumoural fat has been attributed by Ferrozzi et al.[27] to osseous metaplasia of the non-epithelial tumour stroma, which has been described in some renal-cell carcinomas.[29–31] At present, there do not appear to be any clear imaging features that differentiate these particular ACCs from

angiomyelolipomas, a not uncommon benign adrenal tumour in which macroscopic fat is a hallmark.

The presence of ill-defined margins in relation to lesions is often a sign of their underlying aggressive nature. However, the converse does not necessarily apply; namely, the presence of well-defined margins is not necessarily a sign of benignity, as evidenced by the finding of this feature in 71% (29 of 41) of the tumours in the present study. Twenty-five of these 29 tumours were surrounded to some degree by a thin, well-defined enhancing rim; this feature has previously been seen in both small and large tumours and is considered to be the tumour's capsule.[7,8] This capsule may assist in limiting the risk of adjacent organ invasion; in the present series, only four patients had confirmed local organ involvement despite the large size of the majority of tumours and their close abutment and mass effect on adjacent organs.

In addition to directly invading adjacent organs, ACC may extend into the adjacent vasculature, such as the IVC and renal veins; this is usually accompanied by thrombus.[8–10] IVC thrombus was present in approximately 17% (seven of 41) of the present series on contrast-enhanced CT or surgery, which is similar to the reported incidence (14.3%) in a surgical series,[9] In the present series, as in theirs, IVC extension was more commonly observed with right-sided ACC. The longer length of the left renal vein probably explains this finding. To the authors' knowledge, no case of gonadal thrombus in ACC has been described; tumoural invasion into the left renal vein and extending inferiorly along the gonadal vein was observed on CT images in one of the present patients. This patient underwent an adrenalectomy, and the venous thrombus was also confirmed by surgery and pathology. Thrombus can also extend superiorly into the right atrium.[9,10] Although no right atrial thrombus was observed in the present patients, it is recommended that if ACC is suspected, abdominal imaging should provide adequate visualization of the right atrium in order to detect or exclude the possible presence of extension of IVC thrombus.

In the present series, there were three of 41 (7.3%) histopathologically confirmed cases of metastatic retroperitoneal adenopathy. A limitation of this aspect of the present retrospective study is that retroperitoneal lymph node dissection was not undertaken in all patients, and so the negative status of lymph nodes cannot be confirmed. In previous CT-based studies, metastatic adenopathy has been considered to have been present in zero of 10 (0%) patients,[8] and five of 21 (24%).[7] However, these two studies are limited by the lack of pathological confirmation. In an autopsy series of 31 patients with ACC, metastatic retroperitoneal lymphadenopathy was found in 21 (68%) cases.[32] This, however, may not be representative of the status of patients at the time of their initial presentation, which reflects the present population more closely.

Based on the staging evaluations available in the present study, six of 41 (15%) of patients were encountered with distant metastases, including the liver, lungs, and bone. Other clinical series have reported the presence of distant metastases at the time of presentation in 18–39% of patients.[5] In the above autopsy series of 31 patients with ACC,[32] the incidence of lung, liver, and bone metastases were 71, 42, and 26% respectively; other metastatic sites included the gastrointestinal tract, contralateral adrenal, brain, and pleura. As surgical resection of limited or oligometastatic disease is a distinct management option,[2,4,5] careful staging beyond the abdominal cavity should be undertaken. In the present series, all four patients with liver metastases had the primary ACC on the right side, which contrasts with the observation of Fishman et al.[7] in which eight of their nine hepatic metastases were from left-sided ACC. This probably reflects the small sample sizes of these series, which is inevitable given the rarity of the tumour.

The IV contrast-agent washout characteristics of adrenal lesions are suggested as a method of differentiating adenomas from non-adenomas: notably, most of this work has been undertaken in the context of much smaller indeterminate adrenal lesions than those encountered in the present study.[11–14] Adenomas exhibit rapid enhancement and rapid contrast-agent washout, whereas non-adenomas are considered to have more prolonged and delayed washout. The use of PEW and RPEW thresholds of 60 and 40% on delayed contrast-enhanced CT images has been reported to yield sensitivities and specificities for differentiating of adenomas from non-adenomas of 92–100% and 95–100%, respectively.[11–13] However, little detailed information on the washout behaviour of ACCs is available in these series.

In an analysis of seven ACCs, using a range of post-contrast delay times (7–17 min, mean 9 min), mean RPEW of 21.6% have been reported.[16] In a similar analysis of 11 ACCs, mean PEW of 34 ± 9% and mean RPEW 13 ± 12% have been reported, using delays of 10 min.[15] In the present series, the mean PEW of 50 ± 16.9% and mean RPEW of 26.9 ± 11.4% were slightly higher than reported in these previous studies, which may in part be due to the longer delays utilized in the present study (15 min). The washout characteristics observed in the present study are similar to those of non-adenomas in general, as previously reported, which should assist in most ACCs being correctly classified as non-adenomas, rather than as benign adenomas.

Caoili et al.[14] reported on a patient with ACC who had a PEW value in the expected range of adenomas, namely, of 81% (i.e., greater than the threshold value of 60%) with a 15 min enhancement delay; they considered that this might be because of the small size (3 cm) of the particular tumour and its well-differentiated histology. The present series of 17 tumours included five that had PEW values greater than 60% and three with an RPEW greater than 40% (i.e., in the adenoma range). It was not possible to offer the same possible explanation as in the report of Caoili et al. as the tumours in the present series, which exhibited the above washout characteristics, were relatively large (8–10 cm) and all were moderately or poorly differentiated upon histopathological evaluation. Therefore, contrast-agent washout and morphological characteristics should be used in a complementary manner when assessing adrenal lesions.

There are suggestions that FDG PET may help in the evaluation of indeterminate adrenal lesions. A sensitivity of 100% and specificity of 88% for differentiating ACCs from adenomas has been reported in a study of 43 adrenal adenomas and 22 ACCs, using a cut-off ratio of 1.45 for adrenal to liver maximum standardized uptake value (SUV_{max}).[33] However, larger and wider ranging studies are required to further assess the utility of PET-CT in this setting.

There are several limitations of the present study. First, not all of the tumours were surgically resected; seven were sampled only by biopsy, so the CT findings could not be directly compared with the histopathological results for all patients. Second, because of the retrospective nature of the study, a variety of CT systems and techniques were used and that contrast-agent washout data were not available in all cases. However, the results achieved with this diverse range of CT systems and techniques may actually be more reflective of daily clinical practice. Third, there are likely to be observer differences in the delineation of tumour ROIs, which may influence the quantitative data; this could be investigated in future work.

In conclusion, large size, well-defined margins with a thin enhancement rim, and a central area of low attenuation are typical morphological characteristics of ACCs on CT. The predilection for extension into the IVC may also be a useful clue to the diagnosis of ACC.

Finally, most ACCs can be correctly categorized by using the enhancement-washout values that have previously been used for differentiating adenomas from non-adenomas. However, in larger indeterminate adrenal lesions, the washout criteria of PEW >60% and RPEW >40% may not indicate benignity, particularly if they also demonstrate the above described features.

Acknowledgments

The authors thank Wei Wei for statistical evaluation; Karen F. Phillips, ELS, for editing the manuscript; and Delise H. Herron and Ella F. Anderson for assisting with image preparation. This research is supported in part by the National Institutes of Health through MDAnderson's Cancer Center Support Grant, CA016672.

References

1. United States, National Cancer Society, Biometry Branch. Third national cancer survey: incidence data. Bethesda Washington, U.S. Dept. of Health, Education, and Welfare, Public Health Service, National Institutes of Health. National Cancer Institute; 1975.
2. Patalano A, Brancato V, Mantero F. Adrenocortical cancer treatment. Horm Res. 2009; 71(Suppl 1): 99–104. [PubMed: 19153517]
3. Wajchenberg BL, Albergaria Pereira MA, Medonca BB, et al. Adrenocortical carcinoma: clinical and laboratory observations. Cancer. 2000; 88:711–736. [PubMed: 10679640]
4. Wandoloski M, Bussey KJ, Demeure MJ. Adrenocortical cancer. Surg Clin North Am. 2009; 89:1255–1267. [PubMed: 19836496]
5. Rodgers SE, Evans DB, Lee JE, et al. Adrenocortical carcinoma. Surg Oncol Clin N Am. 2006; 15:535–553. [PubMed: 16882496]
6. Dunnick NR, Heaston D, Halvorsen R, et al. CT appearance of adrenal cortical carcinoma. J Comput Assist Tomogr. 1982; 6:978–982. [PubMed: 7142516]
7. Fishman EK, Deutch BM, Hartman DS, et al. Primary adrenocortical carcinoma: CT evaluation with clinical correlation. AJR Am J Roentgenol. 1987; 148:531–535. [PubMed: 3492881]
8. Ribeiro J, Ribeiro RC, Fletcher BD. Imaging findings in pediatric adrenocortical carcinoma. Pediatr Radiol. 2000; 30:45–51. [PubMed: 10663510]
9. Chiche L, Dousset B, Kieffer E, et al. Adrenocortical carcinoma extending into the inferior vena cava: presentation of a 15-patient series and review of the literature. Surgery. 2006; 139:15–27. [PubMed: 16364713]
10. Kim KH, Park JC, Lim SY, et al. A case of non-functioning huge adrenocortical carcinoma extending into inferior vena cava and right atrium. J Korean Med Sci. 2006; 21:572–576. [PubMed: 16778409]
11. Szolar DH, Kammerhuber FH. Adrenal adenomas and non-adenomas: assessment of washout at delayed contrast-enhanced CT. Radiology. 1998; 207:369–375. [PubMed: 9577483]
12. Blake MA, Kalra MK, Sweeney AT, et al. Distinguishing benign from malignant adrenal masses: multi-detector row CT protocol with 10-minute delay. Radiology. 2006; 238:578–585. [PubMed: 16371582]
13. Park BK, Kim CK, Kim B, et al. Comparison of delayed enhanced CT and chemical shift MR for evaluating hyperattenuating incidental adrenal masses. Radiology. 2007; 243:760–765. [PubMed: 17517932]
14. Caoili EM, Korobkin M, Francis IR, et al. Adrenal masses: characterization with combined unenhanced and delayed enhanced CT. Radiology. 2002; 222:629–633. [PubMed: 11867777]
15. Szolar DH, Korobkin M, Reittner P, et al. Adrenocortical carcinomas and adrenal pheochromocytomas: mass and enhancement loss evaluation at delayed contrast-enhanced CT. Radiology. 2005; 234:479–485. [PubMed: 15671003]
16. Slattery JM, Blake MA, Kalra MK, et al. Adrenocortical carcinoma: contrast washout characteristics on CT. AJR Am J Roentgenol. 2006; 187:W21–W24. [PubMed: 16794135]
17. Lee IJ, Lee JM, Kim SH, et al. Helical CT evaluation of the preoperative staging of gastric cancer in the remnant stomach. AJR Am J Roentgenol. 2009; 192:902–908. [PubMed: 19304693]

18. Habermann CR, Weiss F, Riecken R, et al. Preoperative staging of gastric adenocarcinoma: comparison of helical CT and endoscopic US. Radiology. 2004; 230:465–471. [PubMed: 14752188]
19. Copeland PM. The incidentally discovered adrenal mass. Ann Intern Med. 1983; 98:940–945. [PubMed: 6344711]
20. Terzolo M, Ali A, Osella G, et al. Prevalence of adrenal carcinoma among incidentally discovered adrenal masses. A retrospective study from 1989 to 1994. Gruppo Piemontese Incidentalomi Surrenalici. Arch Surg. 1997; 132:914–919. [PubMed: 9267279]
21. Ctvrtlik F, Herman M, Student V, et al. Differential diagnosis of incidentally detected adrenal masses revealed on routine abdominal CT. Eur J Radiol. 2009; 69:243–252. [PubMed: 18226485]
22. Mansmann G, Lau J, Balk E, et al. The clinically inapparent adrenal mass: update in diagnosis and management. Endocr Rev. 2004; 25:309–340. [PubMed: 15082524]
23. Mantero F, Terzolo M, Arnaldi G, et al. A survey on adrenal incidentaloma in Italy. Study Group on Adrenal Tumors of the Italian Society of Endocrinology. J Clin Endocrinol Metab. 2000; 85:637–644. [PubMed: 10690869]
24. Hamrahian AH, Ioachimescu AG, Remer EM, et al. Clinical utility of noncontrast computed tomography attenuation value (hounsfield units) to differentiate adrenal adenomas/hyperplasias from non-adenomas: Cleveland Clinic experience. J Clin Endocrinol Metab. 2005; 90:871–877. [PubMed: 15572420]
25. Guo YK, Yang ZG, Li Y, et al. Uncommon adrenal masses: CT and MRI features with histopathologic correlation. Eur J Radiol. 2007; 62:359–370. [PubMed: 17532488]
26. Dunnick NR. Hanson lecture. Adrenal imaging: current status. AJR Am J Roentgenol. 1990; 154:927–936. [PubMed: 2108567]
27. Ferrozzi F, Bova D. CT and MR demonstration of fat within an adrenal cortical carcinoma. Abdom Imaging. 1995; 20:272–274. [PubMed: 7620426]
28. Heye S, Woestenborghs H, Van Kerkhove F, et al. Adrenocortical carcinoma with fat inclusion: case report. Abdom Imaging. 2005; 30:641–643. [PubMed: 15688105]
29. Strotzer M, Lehner KB, Becker K. Detection of fat in a renal cell carcinoma mimicking angiomyolipoma. Radiology. 1993; 188:427–428. [PubMed: 8327690]
30. Helenon O, Chretien Y, Paraf F, et al. Renal cell carcinoma containing fat: demonstration with CT. Radiology. 1993; 188:429–430. [PubMed: 8327691]
31. Radin DR, Chandrasoma P. CT demonstration of fat density in renal cell carcinoma. Acta Radiol. 1992; 33:365–367. [PubMed: 1633049]
32. Didolkar MS, Bescher RA, Elias EG, et al. Natural history of adrenal cortical carcinoma: a clinicopathologic study of 42 patients. Cancer. 1981; 47:2153–2161. [PubMed: 7226109]
33. Groussin L, Bonardel G, Silvera S, et al. 18F-fluorodeoxyglucose positron emission tomography for the diagnosis of adrenocortical tumors: a prospective study in 77 operated patients. J Clin Endocrinol Metab. 2009; 94:1713–1722. [PubMed: 19190108]

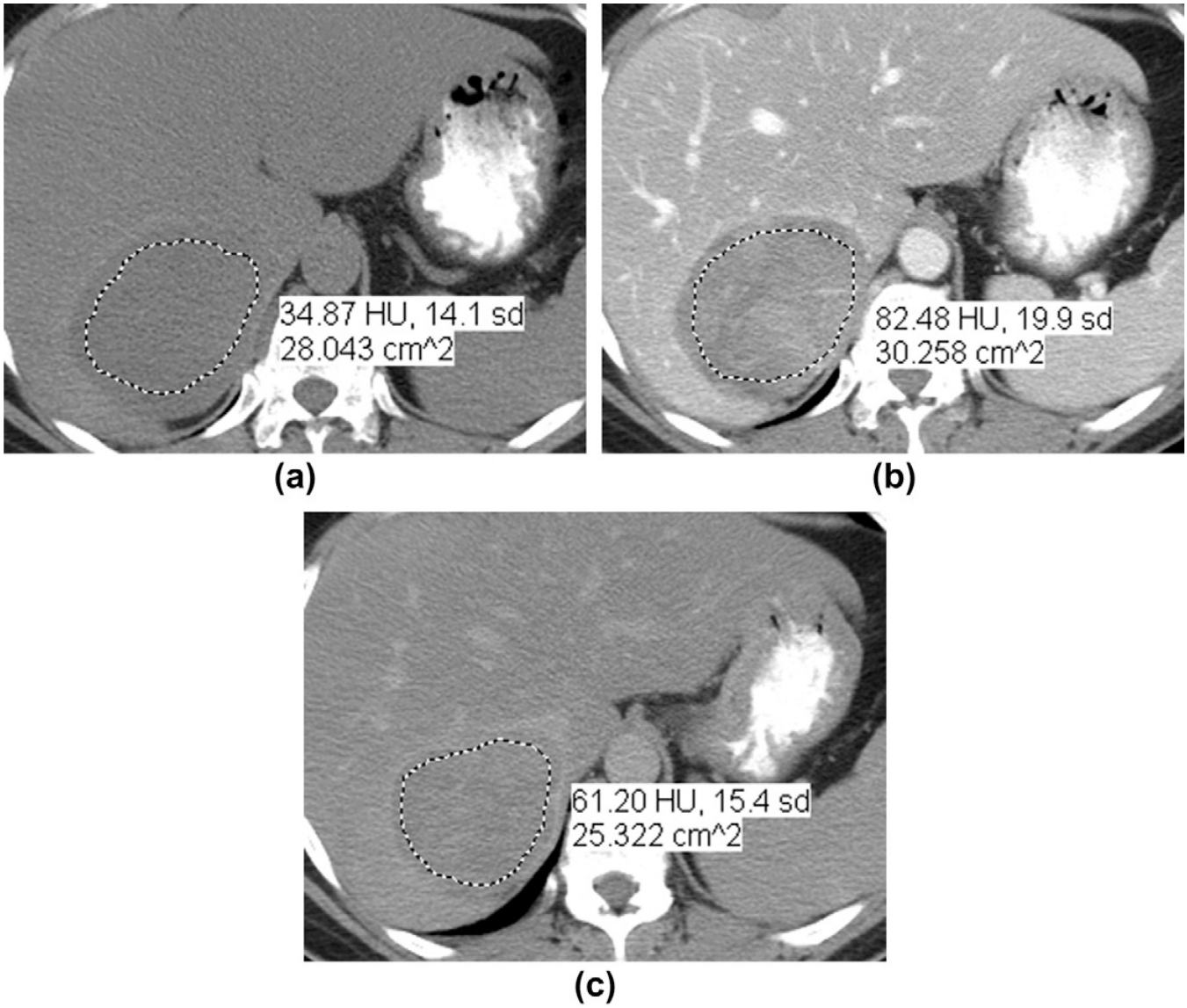

Figure 1.

A 51-year-old woman with a right ACC. (a) Non-contrast-enhanced, (b) portal venous phase, and (c) 15 min delayed contrast-enhanced axial CT images. The oval mass had attenuation values of 35, 82, and 61 HU, respectively. The resultant PEW and RPEW values were 44.7 and 25.6%, respectively. The dotted line indicates the hand-drawn region of interest. The posterior aspect of the liver was compressed by the tumour, however, without CT criteria for adjacent organ invasion (which was confirmed at adrenalectomy). There was no liver invasion on pathology.

Figure 2.
A 42-year-old man with right ACC. Contrast-enhanced CT image shows a 13 cm, well-circumscribed, lobulate mass with irregular calcifications (thin white arrow) and a central stellate area of low density (thin black arrow). The adjacent liver parenchyma and the IVC (thick white arrow) are displaced anteriorly.

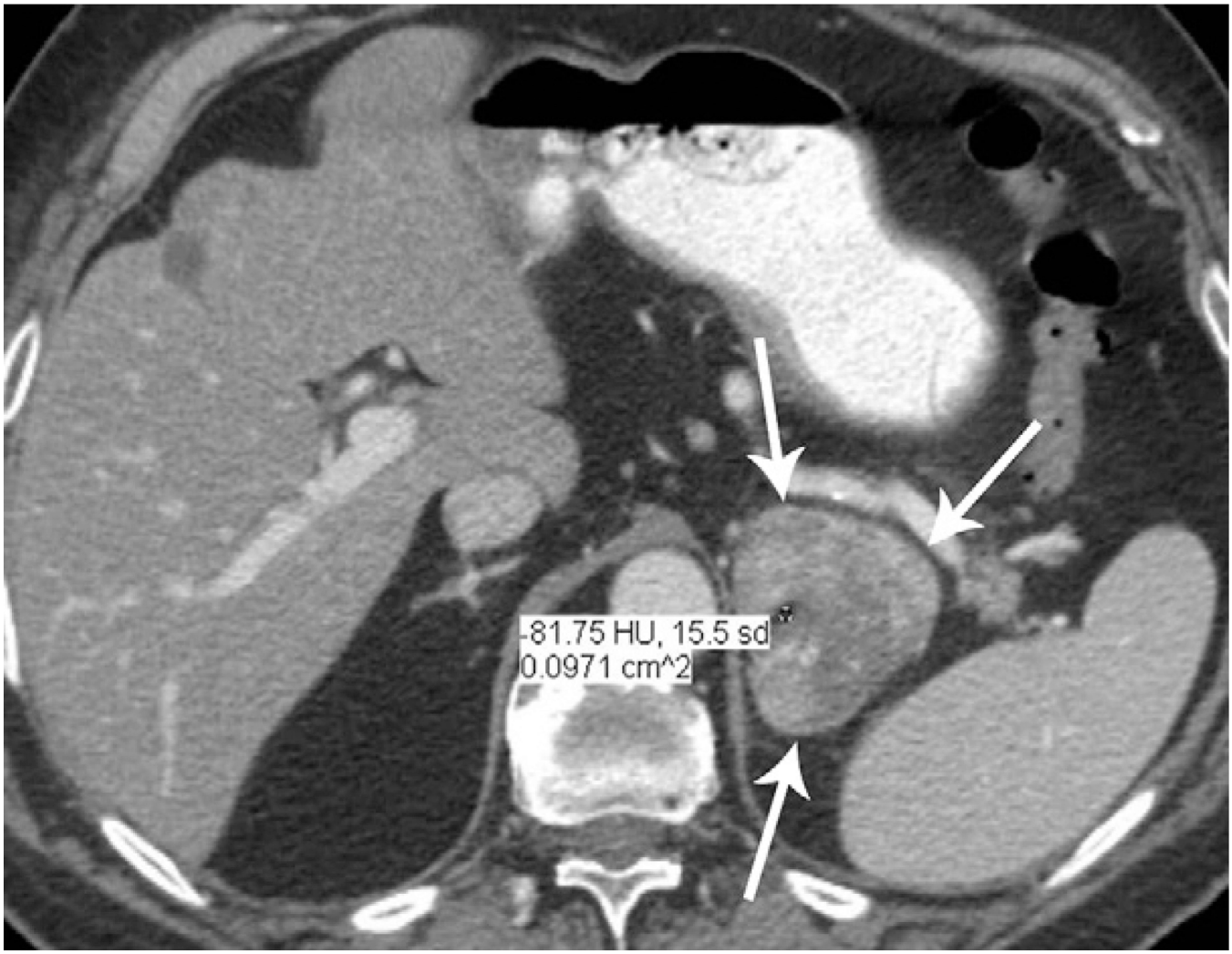

Figure 3.
An 80-year-old man with left ACC. Contrast-enhanced CT image shows a well-defined, lobulate mass containing a small amount of fat (attenuation −81 HU). A thin, capsule-like enhancing rim is visible around the mass (arrows).

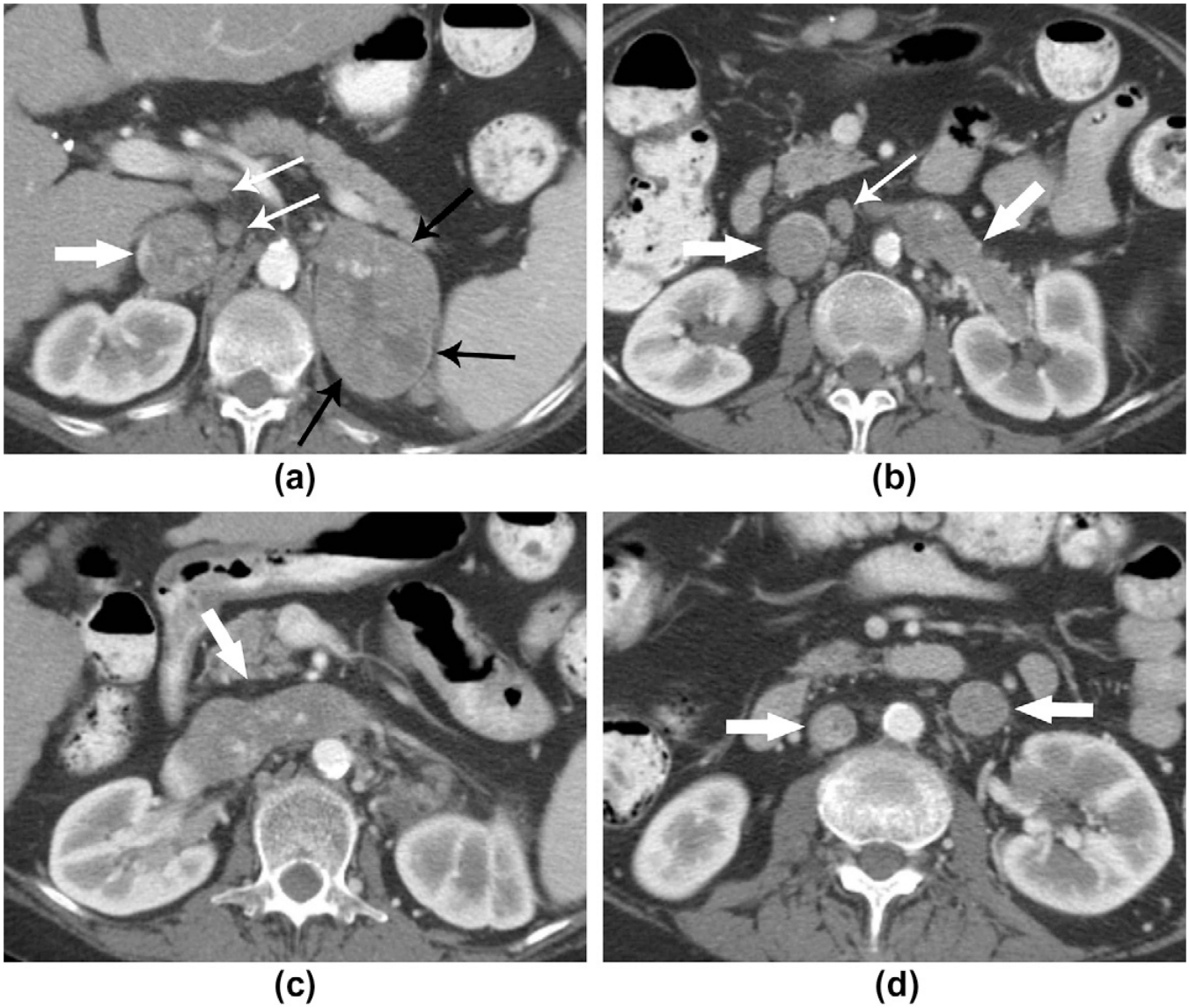

Figure 4.
A 67-year-old woman with left ACC. (a–c) CT images show a well-defined mass with heterogeneous contrast enhancement and a central area of hypodensity arising from the left adrenal gland. Thin enhancing rim (black arrows), tumoural extension into the left renal vein and IVC (thick white arrows). Several enlarged retroperitoneal lymph nodes (thin white arrows) were detected and histopathologically confirmed to be metastases. (d) The image shows the thrombus in the left renal vein extending inferiorly into the left gonadal vein. The IVC thrombus is still visible in this image (thick white arrows).

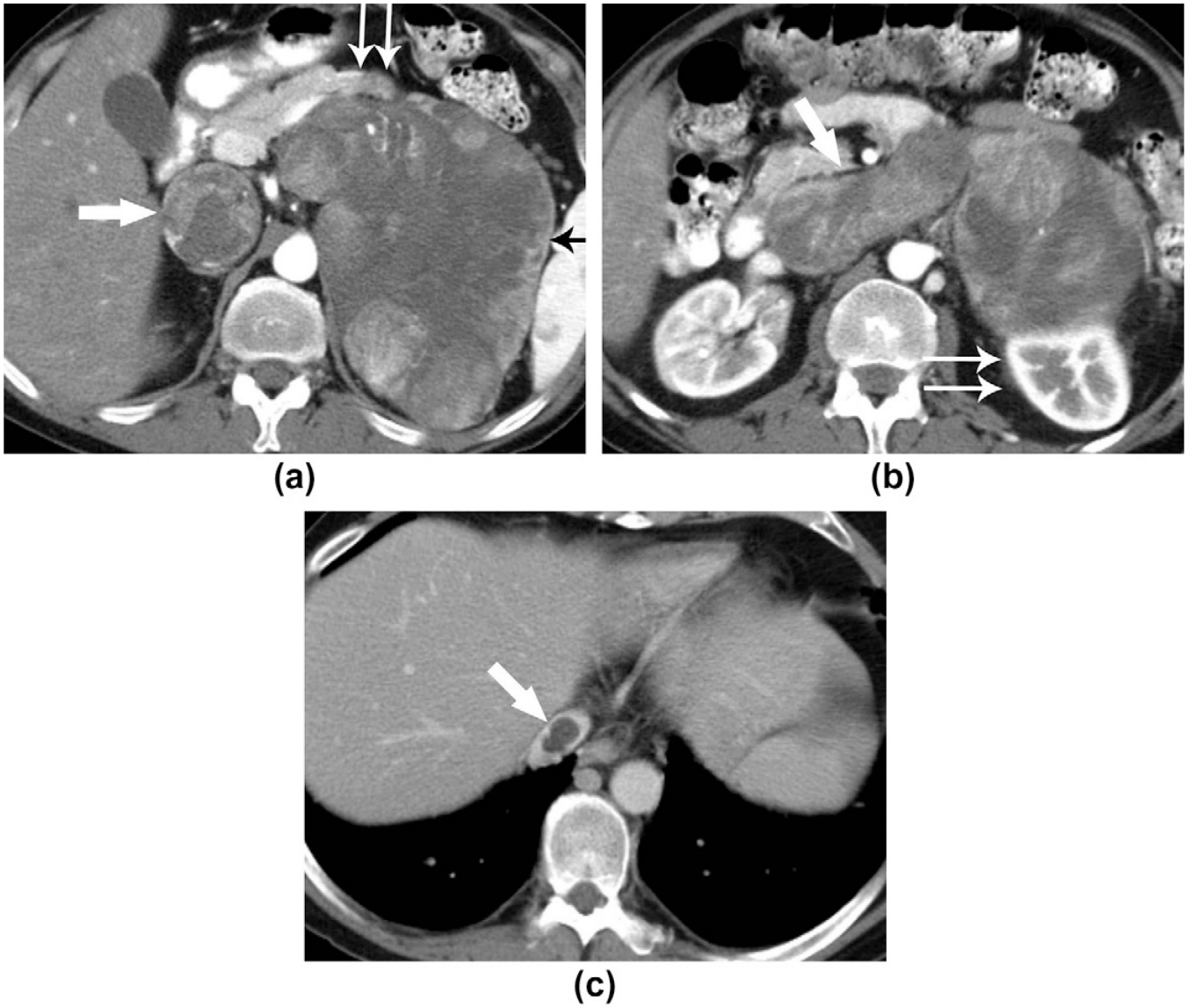

Figure 5.

A 51-year-old man with left ACC. (a, b) CT images show a large lobulate mass arising from the left adrenal gland with a central stellate area of hypodensity and a thin enhancing capsule (black arrow). The body and tail of the pancreas were displaced anteriorly by the mass, and the left kidney was displaced posteriorly and inferiorly (thin white arrows). The tumour extended into the left renal vein and across the midline, extending along the inferior vena cava and (c) superior to the confluence of the hepatic veins (thick white arrows).

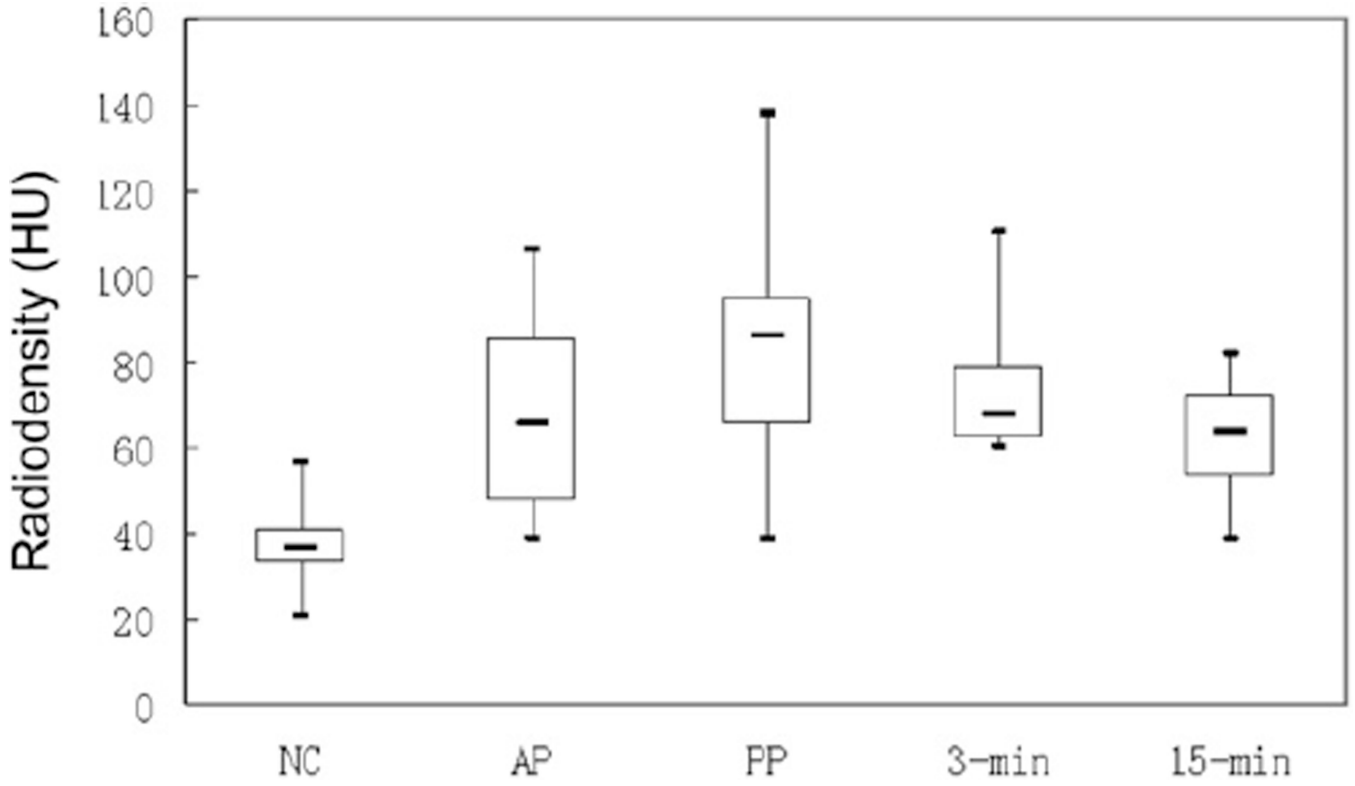

Figure 6.

Box-plot shows attenuation values for ACC on unenhanced (NC) and subsequent phase of IV contrast enhancement. The bold horizontal lines represent medians, the boxes the inter-quartile range, and whiskers indicate minimal and maximum values. NC, unenhanced; AP, arterial phase; PP, portal phase; 3-min, 3 min delay; 5-min, 5 min delay.

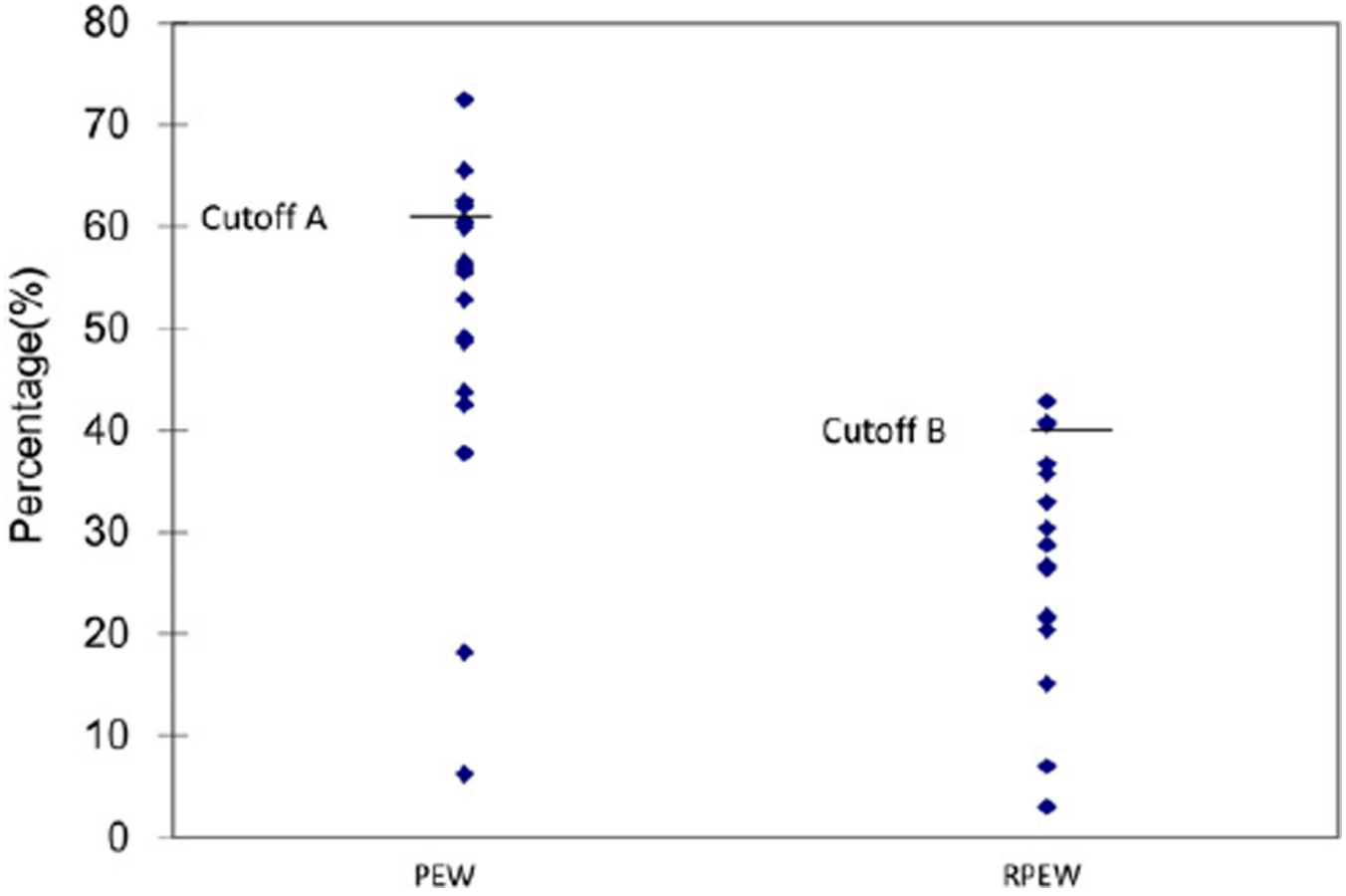

Figure 7.
Scatter-plot shows distribution of PEW and RPEW values for ACCs. “Cut-off A” is 60% and “cut-off B” is 40%, which are the PEW or RPEW thresholds commonly used in previous studies for distinguishing between adrenal adenomas and non-adenomas.[11–13]

Table 1

Relationship between maximal diameter of the 41 adrenocortical carcinomas and the other tumour characteristics evaluated using computed tomography (CT).

Tumour characteristic	Maximal diameter of tumours (cm)					
	Total	≤6	6.1–9	9.1–12	12.1–15	≥15.1
No. of tumours by size	41	3	16	7	8	7
Shape						
Round or oval	11 (27%)	1	5	1	1	3
Lobulate	30 (73%)	2	11	6	7	4
Margin						
Well defined	29 (71%)	3	14	4	6	2
Ill defined	12 (29%)	0	2	3	2	5
Rim enhancement	25 (64%)[b]	2	14	3	5	1
Calcification	15 (37%)	1	4	2	4	4
Shape of central hypodensity						
Stellate	21 (51%)	1	6	2	5	7
Irregular	20 (49%)	2	10	5	3	0
Crossing midline	2 (5%)	0	0	0	0	2
Adjacent organ invasion						
Liver	4 (10%) [1] {1}	0 [1]	1	0	1 [1]	2
Kidney	4 (10%) [2]	0	0	0	0	4 [2]
Pancreas	1 (2%) [1]	0	0	1 [1]	0	0
Stomach	1 (2%) [1]	0	0	1 [1]	0	0
Diaphragm	1 (2%) [1]	0	0	1 [1]	0	0
Venous thrombus						
Inferior vena cava	6 (15%) [3] {1}	0	1 [1] {1}	1	1 [1]	3 [1]
Renal vein	2 (5%) [2]	0	1 [1]	0	0	1 [1]
Gonadal vein	1 (2%) [1]	0	1 [1]	0	0	0
Lymphadenopathy	4 (10%) [2] {1}	0	1 [1]	1 [1]	2	0 {1}
Visceral metastases						
Liver	4[a] (10%) [2]	0	0	1	1 [1]	2 [1]

Tumour characteristic	Maximal diameter of tumours (cm)					
	Total	≤6	6.1–9	9.1–12	12.1–15	≥15.1
Lung	2 (5%)	0	0	1	0	1
Bone	1[a] (2%)	0	0	1	0	0

Totals relate to findings at CT. () = Percent of total of 41 patients, unless otherwise stated; [] = number of cases with findings on CT confirmed surgically and/or histopathologically; {} = number of cases with findings not identified on preoperative CT, but found at surgery, i.e., false-negative CT.

[a] One patient had both liver and bone metastases.

[b] Based on 39 cases with contrast-enhanced CTs.